Octagonal continued fraction and diagonal changes

MAURO ARTIGIANI

ABSTRACT. *In this note we show that the octagon Farey map introduced by Smillie and Ulcigrai in [9, 10] is an acceleration of the diagonal changes algorithm introduced by Delecroix and Ulcigrai in [2].*

1. Introduction

The theory of continued fractions is a beautiful page of mathematics which connects number theory, (hyperbolic) geometry and dynamical systems. Given a number $\alpha \in \mathbb{R}$, its continued fraction expansion is an expression of the form

$$\alpha = [a_0; a_1, a_2, \dots] = a_0 + \cfrac{1}{a_1 + \cfrac{1}{a_2 + \dots}},$$

where $a_0 \in \mathbb{Z}$ and $a_i \in \mathbb{N}$, for $i \neq 0$. The rational approximations $p_n/q_n = [a_0; a_1, \dots, a_n]$ obtained by truncating the continued fraction at level n are called *convergents* and are the best approximations to the number α, among the ones with denominator bounded by q_n. Subtracting the integer part of α, we can assume that $\alpha \in [0, 1]$. The continued fraction of α can then be obtained from the itinerary of the Gauss map $G(x) = \left\{ \frac{1}{x} \right\}$ on $(0, 1]$ and $G(0) = 0$, where $\{\cdot\}$ denotes the fractional part

$$a_i = n \iff G^{i-1}(x) \in \left(\frac{1}{n+1}, \frac{1}{n} \right].$$

The continued fraction algorithm can be also realized in a geometric fashion in the following way, see the introduction of [2] for more details. Having chosen $\alpha \in \mathbb{R}_+ \setminus \mathbb{Q}$, we draw the line in direction $(\alpha, 1)$. Then we consider the basis of $\mathbb{Z}^2$ given by the vectors $e_{-2} = (0, 1)$ and $e_{-1} = (1, 0)$. Note that the line in direction $(\alpha, 1)$ is contained in the cone generated by the vectors e_{-1} and e_{-2}. At each step $n \geq 0$, we are going to replace e_{n-2} with a new vector e_n obtained
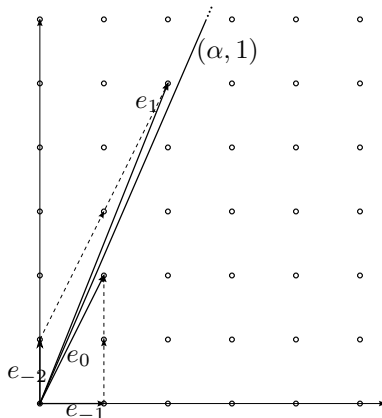
Figure 1: The geometric construction of the convergents of $\alpha \in \mathbb{R}_+$.

by adding to the vector e_{n-2} the vector e_{n-1} as many times as we can *without* crossing the line in direction $(\alpha, 1)$, see Figure 1. In other words

$$e_n = a_n e_{n-1} + e_{n-2}.$$

This shows that, after the step $n = 1$ when we have replaced both our starting vectors, the algorithm is selecting the points in the integer lattice $\mathbb{Z}^2$ that are the closest ones to the line $(\alpha, 1)$ up to their given height. Moreover, it follows from the construction that at each step e_n and e_{n-1} form a basis of $\mathbb{Z}^2$ and that the line in direction $(\alpha, 1)$ is contained in the cone generated by them.

One can show that this procedure produces the continued fraction of $\alpha = [a_0; a_1, \dots]$ and that, if $e_n = (p_n, q_n)$, then p_n/q_n is the nth convergent to α.

It is worth to mention that intermediate vectors of the form $ie_{n-1} + e_{n-2}$, for $i = 1, \dots, a_n - 1$ are also of interest. In fact they yield the additive continued fraction convergents, that is the ones produced by the Farey map, whose acceleration gives the Gauss map itself. These intermediate convergents are called *approximations of the first kind* in the literature, see [4].

It is well-known that the classical continued fraction algorithm acts as a *renormalizing operator* on irrational rotations of the unit interval. It is easy to see that the induced transformation on a Poincaré section of the geodesic flow in an irrational direction on the flat torus $\mathbb{T}^2 = \mathbb{R}^2/\mathbb{Z}^2$ is an irrational rotation. Hence, one can use the Gauss map to renormalize the geodesic flow on the flat torus. From a different point of view, the continued fraction arises from a Poincaré section for the geodesic flow on the moduli space of flat tori, which is (the unit tangle bundle to) a hyperbolic surface, see [7].

Translation surfaces are higher genus analogues of flat tori, defined by gluing a set of polygons in the plane via translations, see Section 2. Translation

surfaces carry a Euclidean structure, hence the geodesic flow on any such surface is given, as in the case of the torus, by a straightline flow in a fixed direction. It is easy to see that the first return map to a transversal for the straightline flow is an interval exchange transformation, which are a generalization of rotations.

It is natural to generalize the theory of continued fractions to translation surfaces. One way to do this is via Rauzy-Veech induction on interval exchange transformations, see [12, 13]. Another point of view, which is a direct generalization of the flat geometric point of view on continued fraction described at the beginning of this introduction, has been taken by Delecroix and Ulcigrai in [2] and their *diagonal changes algorithm* for translation surfaces living in the *hyperelliptic component*. We will recall the basic definitions of diagonal changes in Section 4 below.

A particular family of translation surface is the one of *Veech surfaces* (also called lattice surfaces), originally discovered in [11]. Examples of Veech surfaces are the surfaces obtained from gluing opposite sides of a regular $2n$-gon in the plane by translation. By definition, the moduli space of affine deformations of a Veech surface is also (the unit tangle bundle to) a hyperbolic surface. Hence, one can use methods inspired by hyperbolic geometry, such as the classical ones by Bowen and Series in [1, 8], to code the geodesic on the moduli space of affine deformations of a Veech surface and deduce a continued fraction algorithm from this construction.

Using this point of view Smillie and Ulcigrai have introduced in [9, 10] a continued fraction algorithm for the translation surface obtained from the regular octagon (and more generally for all regular $2n$-gons). Their algorithm can be used to study the straightline flow on the regular octagon from a symbolic point of view, and comes from a particular section of the geodesic flow on the moduli space of affine deformations of the regular octagon. A nice feature of their algorithm is that, unlike the ones defined by Bowen and Series, behaves as a *full shift* on 7 symbols, apart from the first move.

On the surface obtained by gluing opposite sides of a regular octagon in the plane by translation, both the diagonal changes algorithm and the Smillie-Ulcigrai algorithm can be used. Since they are both generalization of the classical continued fraction algorithm on the torus, it is natural to ask whether they are related or not. The content of this note is to show that indeed they are.

THEOREM 1.1. *The octagon additive continued fraction algorithm defined in [10] is an acceleration of the diagonal changes algorithm for the octagon itself.*

Since, as we remarked above, the continued fraction on the octagon is morally a full-shift, this result allows, to a great extent, to bypass the combinatorial complexity of the diagonal changes algorithm, restricting the analysis to a family of loops in the graph of the induction corresponding to the basic moves of the Smillie-Ulcigrai algorithm.

Before concluding this introduction, let us comment on our main result. The Smillie-Ulcigrai algorithm can be defined also on the surfaces obtained by gluing a regular $2n$-gon, forn $n \geq 3$. On these surfaces, one can perform diagonal changes as well. The analogue of Theorem 1.1 remains true for regular $2n$-gon. Similarly to the treatment given in [10], we decided to focus on the case of the octagon in the spirit of concreteness and clarity of exposition, since in this case we can deduce our result by simple geometric considerations. At the end of this paper we briefly sketch how one can generalize our main result to the case of general $2n$-gons.

We remark that is an open question to characterize the behavior of diagonal changes on a Veech surface.

Organization of the paper

In Section 2 we recall the definitions we need about translation surfaces. Then we proceed to describe the additive continued fraction algorithm defined in [9, 10]. In Section 4 we recall the definitions for diagonal changes, and we give a different combinatorial description for the octagon, which is more suited for our discussions. Finally in Section 5 we show Theorem 1.1 and in Section 6 we sketch how to generalize this result to the more general situation of regular $2n$-gons. The drawings needed are included in an Appendix at the end of the document.

2. Definitions

We now introduce the basic definitions on translations surfaces which will be needed in the next sections. General reference on the subject are [3, 6, 13].

A compact *translation surfaces* is a finite collection of polygons $\{P_1, \ldots, P_n\}$ embedded in the plane $\mathbb{R}^2 \cong \mathbb{C}$ together with side identifications as follows. Every side $s_i \in P_i$ is identified with a unique side $s_j \in P_j$ such that the sides s_i and s_j are parallel and have the same length. Moreover, the outward pointing normal vectors with respect to the two sides point in opposite directions. We then identify the sides s_i and s_j by translations. We denote by X the surface obtained after performing all the gluing.

We remark that the presentation of a translation surface as a collection of polygons is *not* canonical. In fact, two collections that differ by *cut and paste* yield the same surface. More precisely, a "cut" operation means cutting some polygon(s) along a straight line connecting two vertices, recording in the new collection of polygons that those sides that have been created are identified in the quotient; a "paste" operation corresponds to gluing some polygons along sides that are identified in the quotient. Two translation surfaces $X = \{P_1, \ldots, P_n\}$ and $X' = \{P'_1, \ldots, P'_m\}$ are *isomorphic* if there exists

a (finite) sequence of cut and paste operation that transforms the colletion $\{P_1, \ldots, P_n\}$ into $\{P'_1, \ldots, P'_m\}$, with the appropriate side identifications. Cut and paste operations are at the heart of the diagonal changes algorithm, which will be described in Section 4

The surface X inherits the Euclidean structure from $\mathbb{R}^2$ everywhere except in a finite set $\mathscr{S}$, which is contained in the image of the vertices of the polygons. These points are called *conical singularities*. Around a point $s \in \mathscr{S}$ the total angle is $2\pi(k_s + 1)$ for $k_s \in \mathbb{N}$. One has the following Gauss-Bonnet formula for the flat metric on the surface:

$$2g - 2 = \sum_{s \in \mathscr{S}} k_s,$$

where g is the genus of the surface X.

The collection of translation surfaces with the same topology, that is number of singularities and value of conical angle around each of them (and hence the same genus), is called a *stratum* and is denoted $\mathcal{H}(k_1, \ldots, k_n)$. One can show that strata are complex orbifold, not necessarily connected.

Thanks to the Euclidean structure on X, for every angle $\theta \in \mathbb{S}^1$ we have a well-defined concept of linear flow in direction θ, which is given in charts by following lines in direction θ on X. The orbit of a point under the linear flow in direction θ is a geodesic for the flat metric on X. A trajectory of the linear flow that connects two (not necessarily distinct) singularities and contains no singularities in its interior is called a *saddle connection*. To a saddle connection we can associate a *displacement vector* (often called *holonomy vector*), by developing the saddle connection to the plane $\mathbb{R}^2$ and taking the difference of its endpoints. In the following, for simplicity, we will often identify saddle connections with their respective displacement vector. A *separatrix* is a trajectory of the linear flow with only one of its endpoints in a singularity.

There is a natural action by affine diffeomorphisms of $\mathrm{GL}(2, \mathbb{R})$ on translation surfaces, given by acting on the polygons that constitute the surface by linear transformations. As the action of $\mathrm{GL}(2, \mathbb{R})$ preserves parallelism, this descents to an action on the surface itself. One can show that the action is continuous on each stratum (with respect to the orbifold topology). The group of affine diffeomorphisms of a translation surface is called the *Veech group* of X. The Veech group is a discrete subgroup of $\mathrm{SL}_\pm(2, \mathbb{R})$, the matrices with determinant equal to ± 1. A surface is called a *Veech surface* if its Veech group is a lattice inside $\mathrm{SL}_\pm(2, \mathbb{R})$. We remark that we will allow orientation reversing affine diffeomorphisms, as this will allow to use the full dihedral group of the regular octagon in Section 3.

3. The octagon Farey map

In this section we will recall the definition of the octagon Farey map. Our presentation will closely follow the one given in [9].

Let $\mathcal{O} \subset \mathbb{C}$ be a regular octagon. We will use $X = X_{\mathcal{O}}$ to denote the translation surface obtained by gluing opposite parallel sides of the octagon. This surface has genus 2 and a single conical singularity of order 6π, coming from the image of the vertices of $\mathcal{O}$, hence it belongs to the stratum $\mathcal{H}(2)$.

Let $D_8 \in \mathrm{GL}(2, \mathbb{R})$ the dihedral group of $\mathcal{O}$, that is the full group of symmetries of the regular octagon. The octagon Farey map will act as a renormalization operator on $\mathbb{S}^1$, the space of directions of trajectories. Since $-\mathrm{id} \in D_8$, we can restrict our analysis to the upper half Σ_+ of $\mathbb{S}^1$. More precisely Σ_+ is the part corresponding to complex numbers with positive imaginary part. As we are thinking of $\mathbb{S}^1$ as the space of directions, it is more convenient to use angle coordinates $\theta \in [0, 2\pi)$ to parametrize points $z = e^{i\theta}$. In other words the angle θ corresponds to the unit vector $(\cos\theta, \sin\theta)$ in $\mathbb{R}^2$. In this coordinates, Σ_+ corresponds to $\theta \in [0, \pi]$. Another coordinate we are going to use is the inverse slope coordinate u on Σ_+ given by $u = \cot(\theta)$. It is natural in this context to extend u to a map from Σ_+ to $\mathbb{RP}^1 = \mathbb{R} \cup \{\infty\}$ sending the endpoints of Σ_+ to the point at infinity. This coordinate is helpful for us since it allows to conveniently express the action of $\mathrm{GL}(2, \mathbb{R})$ on $\mathbb{S}^1$ simply by Möbius maps in the u coordinate.

We divide Σ_+ into 8 sectors $\overline{\Sigma}_j = \left\{ \theta \in \mathbb{S} : \frac{j\pi}{8} \leq \theta \leq \frac{(j+1)\pi}{8} \right\}$, for $i = 0, \ldots, 7$. The sector $\overline{\Sigma}_0$ is a fundamental domain for the action of D_8 on Σ_+. We denote by $\nu_j \in D_8$ the element mapping linearly each sector $\overline{\Sigma}_j$ onto $\overline{\Sigma}_0$. One can check that these elements are

$$\nu_0 = \begin{pmatrix} 1 & 0 \\ 0 & 1 \end{pmatrix}, \quad \nu_1 = \begin{pmatrix} \frac{1}{\sqrt{2}} & \frac{1}{\sqrt{2}} \\ \frac{1}{\sqrt{2}} & -\frac{1}{\sqrt{2}} \end{pmatrix}, \quad \nu_2 = \begin{pmatrix} \frac{1}{\sqrt{2}} & \frac{1}{\sqrt{2}} \\ -\frac{1}{\sqrt{2}} & \frac{1}{\sqrt{2}} \end{pmatrix}, \quad \nu_3 = \begin{pmatrix} 0 & 1 \\ 1 & 0 \end{pmatrix},$$

$$\nu_4 = \begin{pmatrix} 0 & 1 \\ -1 & 0 \end{pmatrix}, \nu_5 = \begin{pmatrix} -\frac{1}{\sqrt{2}} & \frac{1}{\sqrt{2}} \\ \frac{1}{\sqrt{2}} & \frac{1}{\sqrt{2}} \end{pmatrix}, \quad \nu_6 = \begin{pmatrix} -\frac{1}{\sqrt{2}} & \frac{1}{\sqrt{2}} \\ -\frac{1}{\sqrt{2}} & -\frac{1}{\sqrt{2}} \end{pmatrix}, \nu_7 = \begin{pmatrix} -1 & 0 \\ 0 & 1 \end{pmatrix}.$$

Using these maps, we define a folding map $\mathrm{fold} \colon \Sigma_+ \to \overline{\Sigma}_0$ that sends a point $\theta \in \overline{\Sigma}_j$ to the point $\nu_j(\theta)$ with the linear action of ν_j on the corresponding unit vector $(\cos\theta, \sin\theta)$. The different branches of fold agree on the common endpoints and hence we see that fold is a continuous, piecewise linear, map.

Consider now the element

$$\gamma = \begin{pmatrix} -1 & 2(1 + \sqrt{(2)}) \\ 0 & 1 \end{pmatrix}.$$

One can show that γ and D_8 generate the whole Veech group of X. We remark
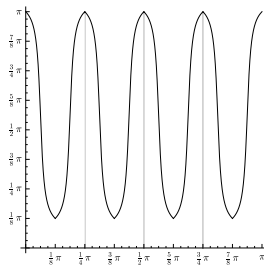
Figure 2: The octagon Farey map in angle coordinates.

that $\gamma^2 = \mathrm{id}$. If we denote with $\overline{\Sigma} = \overline{\Sigma}_1 \cup \cdots \cup \overline{\Sigma}_7$, we see that γ maps $\overline{\Sigma}_0$ to $\overline{\Sigma}$, and vice versa, reversing the orientation.

Call $F_i \colon \overline{\Sigma}_i \to \mathbb{RP}^1$ the map induced by $\gamma\nu_i$. We define the *octagon Farey map* $F \colon \mathbb{RP}^1 \to \mathbb{RP}^1$ to be the map that acts on directions belonging to the sector $\overline{\Sigma}_i$ as F_i. In other words $F = \gamma \circ \mathrm{fold}$, see Figure 2. This, in turn, implies that F is a continuous map. As we said above, the action of F is expressed in the inverse slope coordinate u simply by Möbius transformation: if $u \in \overline{\Sigma}_i$ we have

$$F(u) = \gamma\nu_i * u = \frac{au + b}{cu + d}, \qquad \text{where} \qquad \gamma\nu_i = \begin{pmatrix} a & b \\ c & d \end{pmatrix}$$

The action in the angle coordinate is obtained by conjugation with cot. In the θ coordinate the map F is expanding at every point, except at the endpoints of each sector, but the amount of expansion is not uniform and tends to one at the endpoints of each sector. Since all F_i are monotonic, we can define their inverses $F_i^{-1} \colon \overline{\Sigma} \to \overline{\Sigma}_i$, for $i = 0, \ldots, 7$.

We are now ready to recall the definition of an additive continued fraction algorithm, exploiting the map F. Take a direction $\theta \in [0, \pi]$ and record its *itinerary* $\{s_k\}_{k \in \mathbb{N}}$ under the map F. In other words, we write $s_k = j$ if and only if $F^k(\theta) \in \overline{\Sigma}_j$. This itinerary is unique if $F^k(\theta)$ never coincides with the endpoint of two sectors. We remark that, as the image of F is contained in $\overline{\Sigma}$, only s_0 can be 0. On the other hand, given a sequence $\{s_k\}_{k \in \mathbb{N}}$ of entries $0, \ldots, 7$ such that $s_k = 0$ implies $k = 0$, we consider the intersection $\cap_{k \in \mathbb{N}} F_{s_0}^{-1} F_{s_1}^{-1} \ldots F_{s_k}^{-1} [\frac{\pi}{8}, \pi]$. One can show that the intersection is non empty and consists of only one point. We hence write

$$\theta = [s_0; s_1, s_2, \ldots]_{\mathcal{O}} := \bigcap_{k \in \mathbb{N}} F_{s_0}^{-1} F_{s_1}^{-1} \ldots F_{s_k}^{-1} \left[\frac{\pi}{8}, \pi \right], \tag{1}$$

for an *octagon Farey expansion* of θ.

One direction θ can have at most two expansions. In fact, let us call *terminating* a direction whose continued fraction entries s_k are eventually all 1 or 7.

Then, all points that are not endpoints of a sector $\overline{\Sigma}_j$ have a unique expansion. More precisely, the two sequences $(\ldots, s_k, 1, 1, 1, \ldots)$ and $(\ldots, s_k+1, 1, 1, 1, \ldots)$ correspond to the same direction if s_k is even and $(\ldots, s_k, 7, 7, 7, \ldots)$ and $(\ldots, s_k+1, 7, 7, 7, \ldots)$ correspond to the same direction if s_k is odd. Finally 0 corresponds to $[0; 7, 7, 7, \ldots]_{\mathcal{O}}$ and $\pi = [7; 7, 7, 7, \ldots]_{\mathcal{O}}$.

Since each $\gamma\nu_i$ maps the corresponding sector $\overline{\Sigma}_i$ onto $\overline{\Sigma}$, we want to think of the octagon Farey map F as a *renormalization scheme* acting on directions $\theta \in [0, \pi]$. To illustrate what we mean by this, let us consider a direction θ and let us suppose that its first entry in the octagon Farey expansion is not zero. Then θ belongs to some $\overline{\Sigma}_i \subset \overline{\Sigma}$. Apply F to θ hence corresponds to apply the map $F_i = \gamma\nu_i$, which opens up the sector $\overline{\Sigma}_i$ onto the union of possible sectors $\overline{\Sigma}$. By construction, $F(\theta)$ still belongs to $\overline{\Sigma}$. Moreover, it is clear from (1) that F acts on the Farey expansion of θ as a left shift. In other words, if $\theta = [s_0; s_1, s_2, \ldots]_{\mathcal{O}}$ then $F(\theta) = [s_1; s_2, s_3, \ldots]_{\mathcal{O}}$.

In the following, given a direction $\theta = [s_0; s_1, s_2, \ldots]_{\mathcal{O}}$, we will abuse the notation and continue to call the octagon Farey map the sequence of affine diffeomorphisms given by the octagon continued fraction expansion of θ.

4. The diagonal changes algorithm

4.1. Basic definitions

We are now going to recall the basic definitions of the diagonal changes algorithm, as defined in [2]. For more details and for applications of this algorithm we refer the reader to their original paper.

The diagonal changes algorithm produces a sequence of saddle connections which approximate a given direction $\theta \in \mathbb{S}^1$. These saddle connections from a *wedge*, in the following sense.

DEFINITION 4.1 (Wedges). *A* wedge w *on a translation surface* X *is a pair of saddle connections* $w = (w_l, w_r)$ *such that:*

1. w_l *and* w_r *start from the same conical singularity of* X;

2. w_l *and* w_r *are oriented so that* $\mathrm{Im}(w_l), \mathrm{Im}(w_r) \geq 0$;

3. w_l *is left-slanted (i.e.,* $\mathrm{Re}(w_l) < 0$*) and* w_r *is right-slanted (i.e.,* $\mathrm{Re}(w_r) > 0$*);*

4. (w_l, w_r) *consist of two edges of an embedded triangle in* X.

A *quadrilateral* q in X is the image of an isometrically embedded quadrilateral in $\mathbb{C}$ so that the vertices are singularities of X, and q contains no other singularities.

DEFINITION 4.2 (Admissible quadrangulation). *A quadrilateral q in X is* admissible *if left-slanted and right-slanted saddle connections alternate while we turn around the quadrilateral.*

A quadrangulation Q of X is a decomposition of X into a union of admissible quadrilaterals.

Given a quadrilateral $q \in Q$, let us call the saddle connections that start from the same singularity the bottom sides of q and the ones that end on the same singularities the top sides. We remark that the bottom sides of an admissible quadrilateral, such as one in a quadrangulation of X, form a wedge in the sense of the above definition, which we will call the *base wedge* of q.

Let q be an admissible quadrilateral and $w = (w_l, w_r)$ its base wedge. We say that a q is *left-slanted* if its diagonal is right-slanted. Equivalently, the outgoing vertical separatrix contained in the base wedge of the quadrilateral crosses the top left side. Similarly, we say that a q is *right-slanted* if its diagonal is left-slanted.

A *diagonal change* in an admissible quadrilateral q consists in replacing the base wedge w with a new one. More precisely, if q is left-slanted the new base wedge will be $w' = (w_l, w_d)$, where w_d is the diagonal of q itself. Similarly, if q is right-slanted, the new base wedge will be $w' = (w_d, w_r)$. Remark that in both cases, thanks to our assumption on the slantedness of q the new base wedge still contains a vertical outgoing separatrix. To coherently combine diagonal changes in different quadrilaterals, we will need one more geometrical definition.

DEFINITION 4.3 (Staircases). *Given a quadrangulation Q of X a* left staircase *S for Q (respectively a* right staircase *S for Q) is a subset $S \subset X$ which is the union of quadrilaterals $q_1, \ldots, q_n$ of Q that are cyclically glued so that the top left (resp. top right) side of q_i is identified with the bottom right (resp. bottom left) side of q_{i+1} for $1 \leq i < n$ and of q_1 for $i = n$.*

A left *(respectively* right*) staircase S is* well slanted *if all its quadrilaterals are left (resp. right) slanted.*

DEFINITION 4.4 (Staircase move). *Given a quadrangulation Q and a well-slanted left staircase (respectively a well-slanted right staircase) S, the* staircase move *in X is the operation which consists in doing simultaneously left (resp. right) diagonal changes in all the quadrilaterals of X.*

Having given the basic definitions of the diagonal changes algorithm, we now proceed describing the formalism used to encode it.

DEFINITION 4.5 (Combinatorial datum). *Let Q be a quadrangulation of k quadrilaterals. Let q_i denote the quadrilateral labeled by $i \in \{1, \ldots, k\}$. The* combinatorial datum $\underline{\pi} = \underline{\pi}_Q$ *of the labeled quadrangulation Q is a pair (π_l, π_r) of permutations of $\{1, \ldots, k\}$ such that:*

1. *for each $1 \leq i \leq k$, the top left side of q_i is glued with the bottom right side of $q_{\pi_l(i)}$;*

2. *for each $1 \leq i \leq k$, the top right side of q_i is glued with the bottom left side of $q_{\pi_r(i)}$;*

We remark that, since $w_{i,l}$ and $w_{\pi_l(i),r}$ are the left sides of the quadrilateral q_i and $w_{i,r}$ and $w_{\pi_r(i),l}$ are its right sides, we have

$$w_{i,l} + w_{\pi_l(i),r} = w_{i,r} + w_{\pi_r(i),l}, \qquad \text{for } 1 \leq i \leq k. \tag{2}$$

These equations are called *train-track relations.*

Conversely, we can construct a surface with an admissible quadrangulation, starting with a pair of permutations of k elements $\underline{\pi} = (\pi_l, \pi_r)$ and a length datum

$$\underline{w} = ((w_{1,l}, w_{1,r}), \ldots, (w_{k,l}, w_{k,r})) \in ((\mathbb{R}_- \times \mathbb{R}_+) \times (\mathbb{R}_+ \times \mathbb{R}_+))^k,$$

where $\mathbb{R}_- = \{\, t \in \mathbb{R} : t < 0 \,\}$ and $\mathbb{R}_+ = \{\, t \in \mathbb{R} : t \geq 0 \,\}$. If $\underline{w}$ satisfies the train-track relations (2) we can build a labeled quadrangulation Q that we denote $(\underline{\pi}, \underline{w})$.

We remark that in [2], horizontal vectors are not allowed in a quadrangulation, as this would not allow the definition of a *backward* diagonal changes algorithm However, since we will only use the algorithm forward it will be useful to allow for horizontal saddle connections in the quadrangulation.

4.2. Moves and matrices

Let $Q = (\underline{\pi}, \underline{w})$ be a labeled quadrangulation. For each quadrilateral $q_i \in Q$, let $(w_{i,l}, w_{i,r})$ be its base wedge and call w_d its diagonal, given by

$$w_{i,d} = w_{i,l} + w_{\pi_l(i),r} = w_{i,r} + w_{\pi_r(i),l},$$

where the equality holds thanks to (2). Given a cycle c of a permutation π_r the corresponding staircase S_c formed by the quadrilaterals labeled by the elements of c is well-slanted only if $\mathrm{Re}(w_{i,d}) < 0$ for all $i \in c$, and similarly if c is a cycle of π_l.

Starting from a cycle c of π_r, if its staircase S_c is well-slanted, we can perform a staircase diagonal change as in Section 4.4. The new length data $\underline{w}'$ is given by

$$w_i' = \begin{cases} (w_{i,d}, w_{i,r}), & \text{if } i \in c; \\ w_i, & \text{otherwise.} \end{cases}$$

The new combinatorial datum $\underline{\pi}' = (\pi_l', \pi_r')$ of the new quadrangulation Q' is given by

$$\pi_l'(i) = \begin{cases} \pi_l \circ \pi_r(i), & \text{if } i \in c; \\ \pi_l(i), & \text{otherwise.} \end{cases} \quad \text{and} \quad \pi_r' = \pi_r. \tag{3}$$

Similarly, if c is a cycle of π_l and the corresponding staircase S_c is well-slanted, the new quadrangulation $Q' = (\underline{\pi}', \underline{w}')$ will be given by

$$w_i' = \begin{cases} (w_{i,l}, w_{i,d}), & \text{if } i \in c; \\ w_i, & \text{otherwise.} \end{cases}$$

and

$$\pi_r'(i) = \begin{cases} \pi_r \circ \pi_l(i), & \text{if } i \in c; \\ \pi_r(i), & \text{otherwise.} \end{cases} \quad \text{and} \quad \pi_l' = \pi_l. \tag{4}$$

We remark that the operation on the combinatorial datum does not depend on the length datum and that the operation on the wedges $\underline{w}$ is linear. Hence we can write $\underline{\pi}' = c \cdot \underline{\pi}$, where the action is described above, and we can introduce matrices to encode the action on the length datum. These matrices will be denoted by $A_{\underline{\pi},c} \in \mathrm{SL}(2k, \mathbb{Z})$. Let us index the rows and columns of $A_{\underline{\pi},c}$ with $(1,l), (1,r), \ldots, (k,l), (k,r)$. Denote I_{2k} the $2k \times 2k$ identity matrix and for $1 \leq i, j \leq k$, and $\varepsilon, \nu \in \{l, r\}$ let $E_{(i,\varepsilon),(j,\nu)}$ be the $2k \times 2k$ matrix whose entry in row (i, ε) and column (j, ν) is 1 and all the other entries are 0. We set

$$A_{\underline{\pi},c} = \begin{cases} I_{2k} + \sum_{i \in c} E_{(i,l),(\pi_l(i),r)}, & \text{if } c \text{ is a cycle of } \pi_r; \\ I_{2k} + \sum_{i \in c} E_{(i,r),(\pi_r(i),l)}, & \text{if } c \text{ is a cycle of } \pi_l. \end{cases} \tag{5}$$

Let us summarize the previous discussion.

LEMMA 4.6 (Staircase move on data). *Given a labeled quadrangulation $Q = (\underline{\pi}, \underline{w})$ and a cycle c of $\underline{\pi}$, if the staircase S_c is well slanted, when performing the staircase move in S_c on Q one obtains a new labeled quadrangulation $Q' = (\underline{\pi}', \underline{w}')$ with*

$$\underline{\pi}' = c \cdot \underline{\pi}, \qquad \underline{w}' = A_{\underline{\pi},c} \underline{w},$$

where $c \cdot \underline{\pi}$ and $A_{\underline{\pi},c}$ are given by Equations (3) to (5).

We can construct a graph describing how the combinatorial datum changes using the moves of the diagonal changes algorithm. Following [2], we represent in Figure 3 the graph obtained beginning from $\pi_l = (1, 2)$ and $\pi_r = (2, 3)$. One can show that this graph represents all the possible moves for a surface in $\mathcal{H}(2)$, see [2] for more details. Let us explain the notation used in it. At every vertex we represent the permutation π_l above π_r. Arrows are labeled with words of
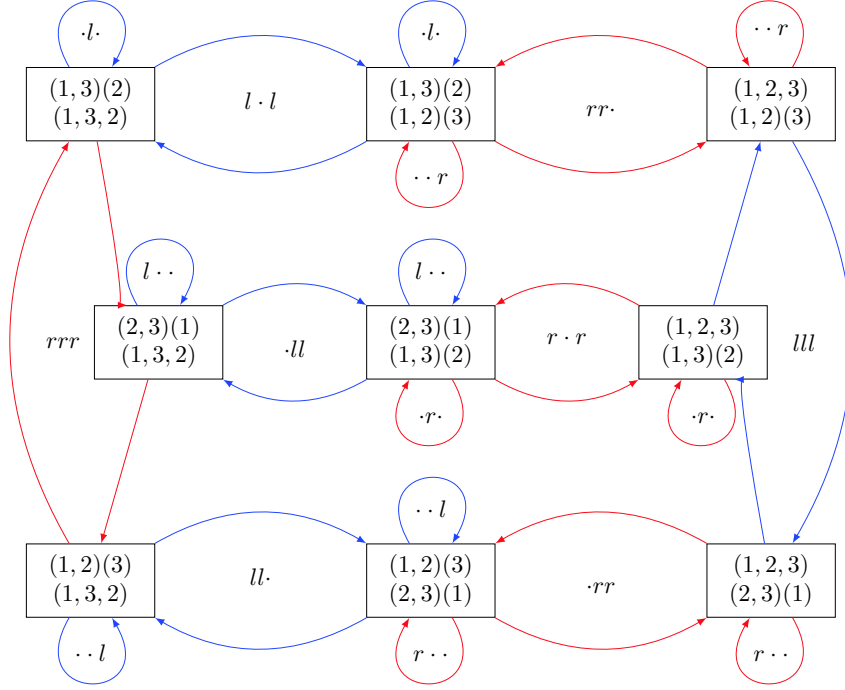
Figure 3: The possible moves in $\mathcal{H}(2)$.

length k representing cycles c in the following way. If $\underline{\pi}'$ is obtained from $\underline{\pi}$ by a left staircase move, that is if c is a cycle for π_l, then the corresponding arrow is labeled by a word with letters in $\{l, \cdot\}$ where the ith letter is equal l if, and only if, $i \in c$. Similarly, if $\underline{\pi}'$ is obtained from $\underline{\pi}$ by a right staircase move, we use letters in $\{r, \cdot\}$.

4.3. A simpler description of diagonal changes in $\mathcal{H}(2)$

A more convenient description, for our purposes, of diagonal changes in $\mathcal{H}(2)$ is given by the following. Let us introduce a move, called *symmetry*, which exchange the left and right vectors in every quadrilateral. Moreover, we allow to relabel the wedges. The graph we obtain is drawn in Figure 4. In fact, allowing relabeling collapses the three rows in Figure 3 into one. The symmetry then identifies the left and right node into a single one which, along with the central one, gives us our reduced graph.

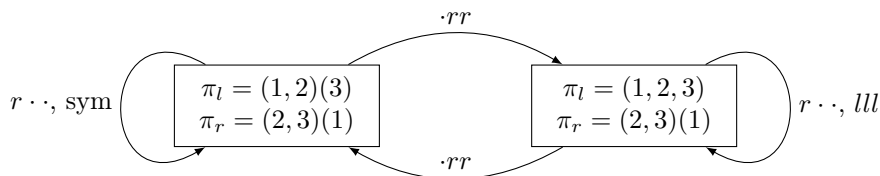We have introduced these extra moves for the following reasons. The oc-

Figure 4: The possible moves in $\mathcal{H}(2)$, up to relabeling and symmetry.

tagonal continued fraction constructed in [9] and recalled in Section 3 uses also orientation reversing affine diffeomorphisms. Hence the symmetry is needed in order to represent via diagonal changes that algorithm, precisely for the moves corresponding to even numbered sectors. Moreover, since the moves of the octagon Farey map act on the unlabeled quadrangulation of the octagon, we need to forego that extra data, that is we have to allow for relabelings. In fact, the (combinations of) moves of the diagonal changes that correspond to the octagon Farey map usually begin at one vertex of the graph of possible moves in $\mathcal{H}(2)$ and end at one which is different from the original one. The starting vertex and the final one differ precisely by a relabeling. Relabeling the wedges hence is needed to make sure that the concatenation of diagonal changes agrees with the action of the octagon Farey map; and also allows us to combine the moves from one step to the next.

In the basis given by $\{E_{(1,l)}, E_{(1,r)}, \ldots, E_{(3,r)}\}$, the moves in Figure 4 are given by the following matrices.

- $\cdot rr$ from the left node to the right one;

- $\cdot rr$ from the right node to the left one;

- $r \cdot\cdot$ (which is the same matrix in both nodes);

- lll plus relabeling;

- the left/right symmetry plus relabeling.

5. The octagon Farey map in terms of diagonal changes

In this section, we show that the octagon Farey expansion is an acceleration of diagonal changes moves, that is we prove Theorem 1.1. Given a direction $\theta = [s_0; s_1, s_2, \ldots]_{\mathcal{O}}$, we have a well-defined sequence of maps $(F_{s_i})_{s_i \in \mathbb{N}}$. These maps act affinely on the surface $X_{\mathcal{O}}$. As we said above, with a slight abuse of notation, we will refer to this sequence of maps also as the octagon Farey map.

5.1. Step 0

In the octagon Farey expansion the first entry s_0 plays a special role, since it is the only case in which we can have $s_i = 0$. By definition, after the 0 step of the algorithm we obtain the sector $F_{s_0}^{-1}[\pi/8, \pi] = \overline{\Sigma}_{s_0}$ of amplitude $\pi/8$ to which the direction θ belongs. Thus, s_0 dictates the starting quadrangulation of the surface $X_{\mathcal{O}}$.

Let Q' be the quadrangulation in Figure 5, formed by wedges in directions π and $\pi/8$. Applying γ to Q' we obtain a new quadrangulation, Q, shown in Figure 6, now in the directions $\pi/8$ and 0, with inverted orientation. Then the beginning quadrangulation of $X_{\mathcal{O}}$ is $Q_0 = \nu_{s_0}^{-1} Q = F_{s_0}^{-1} Q'$.

5.2. Further steps

We now describe how to translate the induced action of the octagon Farey expansion in terms of diagonal changes. We remark that, as s_0 dictates the starting quadrangulation, and the other s_i only take values from 1 to 7, we only have to translate these seven cases.

Renormalizing, we apply the map F_{s_0} to the octagon. As the octagon Farey map acts by a shift, we are now approximating the direction $\theta^{(1)} = F(\theta) = [s_1; s_2, \ldots]_{\mathcal{O}}$. By our choice of initial quadrangulation, we have to produce the wedges bounding the sector $\overline{\Sigma}_{s_1}$ to which $\theta^{(1)}$ belongs, representing them as linear combinations of the ones in the quadrangulation $F_{s_0} Q_0 = Q'$.

Having done this first step, we now renormalize once again, and apply the map F_{s_1} to the surface. Thus, we are back to approximating the direction $\theta^{(2)} = F_{s_1}(\theta^{(1)})$ with respect to the quadrangulation obtained after the diagonal changes and having undone them by applying the Farey map. In other words, we have to approximate a direction in $[\pi/8, \pi]$ with respect to the quadrangulation Q', as we just did.

REMARK 5.1: Another natural choice for a starting quadrangulation would be to begin with the quadrangulation $\widetilde{Q}$ made by the rectangle in the middle of the octagon and by the two trapezes at the top and at the bottom. Then we would apply the map $\nu_{s_0}^{-1}$ to it and obtain our starting quadrangulation of the octagon. Since γ is the composition of a Dehn twist in the horizontal cylinder and the
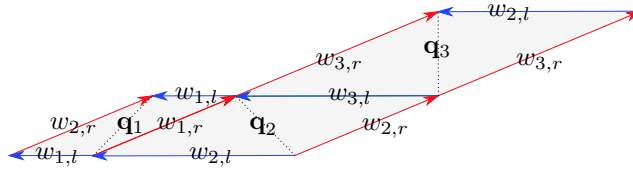

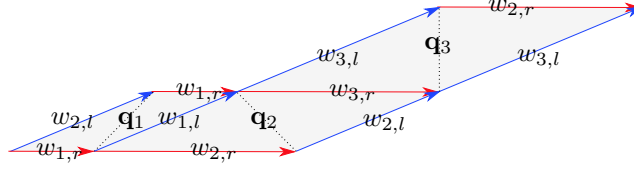Figure 5: The quadrangulation Q' of the regular octagon.

Figure 6: The quadrangulation Q of the regular octagon.

reflection with respect to vertical line, the renormalized quadrangulation $\gamma\widetilde{Q}$ is wider than Q'. This quadrangulation is a configuration as the one in the right of Figure 4. Hence, we can apply the moves $\cdot rr$ and $r\cdot\cdot$ to $\gamma\widetilde{Q}$ and go back to our configuration Q'.

We now proceed to list the sequences of diagonal changes moves which produce the wedges bounding the sectors $\overline{\Sigma}_i$ starting from the quadrangulation Q', thus completing the proof of Theorem 1.1.

In order to perform diagonal changes, we label quadrilaterals in Q' so that the combinatorial datum $\underline{\pi}$ is given by

$$\pi_l = (1,2)(3), \qquad \text{and} \qquad \pi_r = (1)(2,3).$$

Let us remark once again that we will use diagonal changes to approximate the direction $\theta = [s_1; s_2, \ldots]_{\mathcal{O}}$ and *not* the vertical one. Figures that represent the movements can be found at the end of the document, see Appendix A for some comments about them.

1. First sector $\left(\frac{\pi}{8} \leq \theta \leq \frac{2\pi}{8}\right)$: $\cdot rr$, $r\cdot\cdot$, $\cdot rr$, see Figure 8. Hence:

$$A_1 = \begin{pmatrix} 1 & 0 & 0 & 1 & 0 & 0 \\ 0 & 1 & 0 & 0 & 0 & 0 \\ 0 & 1 & 1 & 0 & 0 & 1 \\ 0 & 0 & 0 & 1 & 0 & 0 \\ 0 & 1 & 0 & 0 & 1 & 1 \\ 0 & 0 & 0 & 0 & 0 & 1 \end{pmatrix}.$$

2. Second sector $\left(\frac{2\pi}{8} \leq \theta \leq \frac{3\pi}{8}\right)$: $\cdot rr$, lll, $r\cdot r$, $\cdot r\cdot$, symmetry, see Figure 9. Hence:

$$A_2 = \begin{pmatrix} 1 & 1 & 0 & 0 & 0 & 0 \\ 1 & 0 & 0 & 1 & 1 & 1 \\ 0 & 1 & 1 & 0 & 0 & 1 \\ 1 & 1 & 0 & 0 & 1 & 1 \\ 0 & 0 & 0 & 1 & 1 & 1 \\ 0 & 2 & 2 & 0 & 0 & 1 \end{pmatrix}.$$

3. Third sector $\left(\frac{3\pi}{8} \leq \theta \leq \frac{4\pi}{8}\right)$: $\cdot rr$, lll, lll, $\cdot rr$, see Figure 10. Hence:

$$A_3 = \begin{pmatrix} 0 & 0 & 0 & 0 & 1 & 1 \\ 1 & 1 & 1 & 0 & 0 & 1 \\ 1 & 1 & 1 & 1 & 1 & 1 \\ 1 & 1 & 0 & 0 & 1 & 1 \\ 1 & 2 & 2 & 0 & 0 & 1 \\ 0 & 1 & 1 & 1 & 1 & 1 \end{pmatrix}.$$

4. Fourth sector $\left(\frac{4\pi}{8} \leq \theta \leq \frac{5\pi}{8}\right)$: $\cdot \cdot l$, $\cdot rr$, $\cdot rr$, $ll\cdot$, $ll\cdot$, $r \cdot \cdot$, symmetry, see Figure 11.

These moves correspond in the reduced graph to: symmetry, $r \cdot \cdot$, symmetry, $\cdot rr$, $\cdot rr$, symmetry $\cdot rr$, $\cdot rr$, symmetry, $r \cdot \cdot$, symmetry. Hence:

$$A_4 = \begin{pmatrix} 0 & 0 & 1 & 0 & 0 & 1 \\ 0 & 1 & 1 & 0 & 1 & 1 \\ 1 & 1 & 1 & 1 & 1 & 1 \\ 0 & 1 & 2 & 0 & 0 & 1 \\ 1 & 2 & 1 & 0 & 1 & 1 \\ 2 & 1 & 1 & 1 & 1 & 1 \end{pmatrix}.$$

5. Fifth sector $\left(\frac{5\pi}{8} \leq \theta \leq \frac{6\pi}{8}\right)$: $\cdot \cdot l$, $\cdot rr$, lll, $r \cdot r$, $l \cdot \cdot$, see Figure 12.

These moves correspond in the reduced graph to: symmetry, $r \cdot \cdot$, symmetry, $\cdot rr$, lll, $\cdot rr$, symmetry, $r \cdot \cdot$, symmetry. Hence:

$$A_5 = \begin{pmatrix} 0 & 1 & 1 & 0 & 0 & 0 \\ 0 & 0 & 1 & 1 & 1 & 1 \\ 1 & 1 & 1 & 0 & 1 & 1 \\ 0 & 1 & 2 & 0 & 0 & 1 \\ 1 & 0 & 1 & 1 & 1 & 1 \\ 2 & 2 & 1 & 0 & 1 & 1 \end{pmatrix}.$$

6. Sixth sector $\left(\frac{6\pi}{8} \leq \theta \leq \frac{7\pi}{8}\right)$: $ll\cdot$, $\cdot \cdot l$, rrr, $l \cdot l$, see Figure 13.

These moves correspond in the reduced graph to: symmetry, $\cdot rr$, $r \cdot \cdot$, lll, $\cdot rr$. Hence:

$$A_6 = \begin{pmatrix} 0 & 0 & 0 & 1 & 1 & 0 \\ 1 & 1 & 1 & 0 & 0 & 0 \\ 1 & 1 & 1 & 0 & 1 & 1 \\ 1 & 0 & 0 & 1 & 1 & 0 \\ 1 & 1 & 2 & 0 & 0 & 1 \\ 0 & 0 & 1 & 0 & 1 & 1 \end{pmatrix}.$$

7. Seventh sector $\left(\frac{7\pi}{8} \leq \theta \leq \pi\right)$: $ll\cdot, \cdot\cdot l, ll\cdot, \cdot\cdot l$, see Figure 14.

These moves correspond in the reduced graph to: symmetry, $\cdot rr, r\cdot\cdot, \cdot rr,$ $r\cdot\cdot$, symmetry. Hence:

$$A_7 = \begin{pmatrix} 1 & 0 & 0 & 0 & 0 & 0 \\ 1 & 1 & 0 & 0 & 1 & 0 \\ 0 & 0 & 1 & 0 & 0 & 0 \\ 1 & 0 & 0 & 1 & 1 & 0 \\ 0 & 0 & 0 & 0 & 1 & 0 \\ 0 & 0 & 2 & 0 & 0 & 1 \end{pmatrix}.$$

6. Regular $2n$-gons

In the introduction we sketched how diagonal changes are related to the classical continued fraction algorithm on the torus. The central part of this paper was devoted to the octagon. In this section we briefly sketch how for regular $2n$-gons for $n \geq 3$.

6.1. $2n$-gon Farey expansion

We denote with X_{2n} the surface obtained after gluing opposite sides of the regular $2n$-gon. The cases when $n = 2k$ is even and $n = 2k + 1$ is odd are slightly different. In the first case, X_{2n} has only one conical singularity of total angle $2(n-1)\pi$ and hence lies in $\mathcal{H}(n-2)$. If $n = 2k+1$, the surface has 2 singularities, resulting after identifications of half the vertices of the $2n$-gon. Each of the singularity is of $2k\pi = (n-1)\pi$, and the corresponding stratum is $\mathcal{H}\left(\frac{n-3}{2}, \frac{n-3}{2}\right)$. An example of this can be seen in Figure 7.

The dihedral group D_{2n} of the regular $2n$-gon is generated by the horizontal reflection $\alpha^{(n)}$ and the reflection $\beta^{(n)}$ with respect to the line at angle $\pi/2n$ with the horizontal line. For $i = 0, \ldots, n-1$ we can construct $2n$ angular sectors of amplitude $\frac{\pi}{2n}$:

$$\overline{\Sigma}_i^{(n)} = \left\{ \theta \in \mathbb{S} : \frac{i\pi}{2n} \leq \theta \leq \frac{(i+1)\pi}{2n} \right\}.$$

As before, the sector $\overline{\Sigma}_0^{(n)}$ is a fundamental domain for the action of D_{2n} on Σ^+. For $i = 0, \ldots, n$, we define $\nu_i^{(n)}$ to be the element of D_{2n} such that $\nu_i^{(n)} \overline{\Sigma}_i^{(n)} = \overline{\Sigma}_0^{(n)}$. One can check that

$$\nu_i^{(n)} = (\alpha^{(n)} \beta^{(n)})^i, \quad \text{if } i \text{ is even}, \quad \text{and} \quad \nu_i^{(n)} = (\alpha^{(n)} \beta^{(n)})^i \beta^{(n)}, \quad \text{if } i \text{ is odd}.$$

The regular $2n$-gon can be divided into k horizontal cylinders, that is maximal subsets foliated by periodic horizontal trajectories for the linear flow
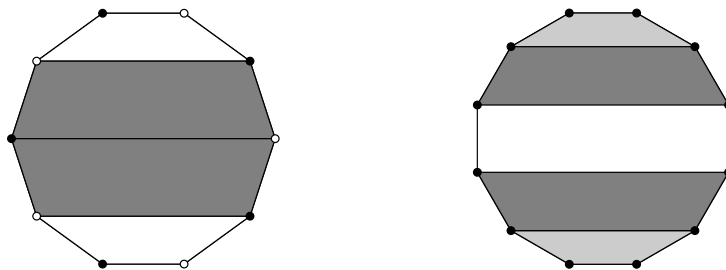
Figure 7: Horizontal cylinders for the regular decagon and the regular 12-gon.

on X_{2n}, see Figure 7. By definition, the boundary of each cylinder is composed of horizontal saddle connections. A cylinder is isometric to $\mathbb{R}/w\mathbb{Z}\times[0,h]$, where w is the length of an horizontal trajectory inside the cylinder and h is the height of the cylinder. The ratio w/h is called the *inverse modulus* of the cylinder. If $n = 2k + 1$, with some simple trigonometry, one can check that the inverse modulus is equal to $\mu^{(n)} = 2\cot\left(\frac{\pi}{2n}\right)$ for all k cylinders. If $n = 2k$, $k - 1$ horizontal cylinders have inverse modulus equal to $\mu^{(n)}$ and the last one has inverse modulus equal to $\mu^{(n)}/2$. In both cases, there is a globally well defined affine diffeomorphism, which acts by a Dehn twist simultaneously on all cylinders in X_{2n}, whose derivative is given by

$$\sigma^{(n)} = \begin{pmatrix} 1 & 2\cot\left(\frac{\pi}{2n}\right) \\ 0 & 1 \end{pmatrix}.$$

Following [11] and [10], one can prove that the Veech group of X_{2n} is generated by D_{2n} and the element $\gamma^{(n)}$ given by

$$\gamma^{(n)} = \sigma^{(n)}\nu_n^{(n)} = \begin{pmatrix} -1 & 2\cot\left(\frac{\pi}{2n}\right) \\ 0 & 1 \end{pmatrix}.$$

Similarly to how we described in Section 3 we can construct a *2n-gon Farey map* defined by

$$F^{(n)}(\theta) = \cot^{-1}(\gamma^{(n)}\nu_i^{(n)}(\cot\theta))$$

if $\theta \in \overline{\Sigma}_i^{(n)}$ for $i = 0, \ldots, n - 1$. Since this map is expanding inside every sector, we can locally invert it and hence construct an associated *2n-gon Farey expansion of* θ, which is now an infinite sequence s_k with $s_0 \in \{0, \ldots, n-1\}$ and $s_k \in \{1, \ldots, n-1\}$ if $k \geq 1$. This expansion is unique with the exception of the sequences that are eventually equal to 1 or to $n - 1$.

6.2. Diagonal changes for the regular $2n$-gons

The regular $2n$-gon is fixed by the rotation by 180 degrees with respect to its center. This induces on the surface X_{2n} an involution, which can be shown to be the *hyperelliptic* involution. We recall that strata of translation surfaces are not necessarily connected and that their connected components have been completely classified in [5]. Diagonal changes are defined for translation surfaces living in the so-called hyperelliptic components, which only exists for the strata $\mathcal{H}(g-1, g-1)$ and $\mathcal{H}(2g-2)$, where $g \geq 2$ is the genus of the corresponding translation surfaces. The surface X_{2n} always belong to such components.

We can decompose X_{2n} into $n-1$ admissible quadrilaterals, on which we can act via the diagonal changes algorithm. However, the combinatorial complexity of the algorithm, and with it the graph describing the combinatorial datum under diagonal changes, similar to the one depicted in Figure 3, grows quite rapidly. To obtain a more manageably sized graph, we can allow for relabeling of the quadrilaterals and introduce a symmetry operation, similarly to what we did to obtain Figure 4. We remark that, if $n = 2k$ the symmetry operation fixes a combinatorial datum, this is *not* the case if $n = 2k+1$. This is a consequence of the structure of the combinatorial datum, which in turn is caused by the fact that if k is even the central horizontal cylinder of the $2n$-gon has a different inverse modulus from the remaining ones and hence plays a special role.

One can repeat the procedure we describe in Section 5 to show that also for a general $2n$-gon the $2n$-gon Farey algorithm is an acceleration of the diagonal changes algorithm. Let us comment a bit more on this.

Given a direction θ, its first digit in the $2n$-gon Farey expansion s_0 dictates the starting quadrangulation of X_{2n}. We define Q' the quadrangulation formed by $n-1$ quadrilaterals given by wedges in direction π and $\pi/2n$. By applying $\gamma^{(n)}$ we obtain a quadrangulation Q formed by wedges in direction 0 and $\pi/2n$. Then the starting quadrangulation of X_{2n} is $Q_0 = (\nu_{s_0}^{(n)})^{-1}Q = (F_{s_0}^{(n)})^{-1}Q'$. This quadrangulation is formed by wedges of amplitude $\pi/2n$ which bound the sector $\overline{\Sigma}_i^{(n)}$ to which the direction θ belongs.

In general, we can label Q' so that the combinatorial datum is given by

$$\begin{pmatrix} \pi_l = (1,2)(3,4)\cdots(n-3,n-2)(n-1) \\ \pi_r = (1)(2,3)\cdots(n-2,n-1) \end{pmatrix}, \quad \text{if } n = 2k,$$

and

$$\begin{pmatrix} \pi_l = (1,2)(3,4)\cdots(n-2,n-1) \\ \pi_r = (1)(2,3)\cdots(n-3,n-2)(n-1) \end{pmatrix}, \quad \text{if } n = 2k+1.$$

We can now renormalize by applying the map $F_{s_0}^{(n)}$ to X_{2n} and approximate the direction $\theta' = F^{(n)}(\theta)$. We are now left to represent the wedges bounding the sector $\overline{\Sigma}_{s_i}^{(n)}$, to which θ' belongs, in terms of the ones in Q'. In principle,

one could repeat the analysis we carried to explicitly find the description in terms of diagonal changes corresponding to the action on every sector of the $2n$-gon Farey expansion. Unfortunately, we were not able to find a closed combinatorial description for these moves. Nevertheless, playing with the cases of the hexagon, octagon, decagon and dodecagon, we discovered some patterns, which could be useful towards this kind of description.

- The moves corresponding to the first sector correspond to applying once the right diagonal change in the quadrilateral labelled by 1, which forms a right staircase by itself, and twice the right diagonal changes in all the remaining right staircases.

- Similarly, but not identically, the moves corresponding to the last sector correspond to applying twice the left diagonal change in all the left staircases.

- The moves corresponding to the middle sector $\overline{\Sigma}_n^{(n)}$ has the following pattern:

  - if $n = 2k$ we do one left move in the quadrilateral labelled by $n - 1$, we do two right moves in the staircase $(n - 3, n - 2)$, we do two left moves in the staircase $(n - 4, n - 3)$, we do two right moves in the staircase $(n - 3, n - 2)$, ..., we do two left moves in the staircase $(1, 2)$, and finally we do one right move in the quadrilateral 1.
  - if $n = 2k + 1$, the moves are as in the case when n is even, exchanging the roles of left and right.

- The number of left moves increases by 1 when increasing the sectors, from the first to the middle one. Similarly the number of right moves decreases by 1 when decreasing the sectors, from the last to the middle one.

- The pattern of the moves corresponding to the sectors from 1 to $n - 1$ of a $2n$-gon seems to pass on to the pattern of the moves corresponding sectors for the $(2n+2)$-gon. Similarly for the sectors from $n+1$ to $2n-1$.

These patterns can be seen in Tables 1 and 2, which we include to help further investigations on this matter.

Acknowledgments

Table 1: The moves for the regular hexagon, octagon and decagon.

Sector	Hexagon	Octagon	Decagon
1	$r\cdot, \cdot r, \cdot r$	$r\cdot\cdot, \cdot rr, \cdot rr$	$r\cdot\cdot\cdot, \cdot rr\cdot, \cdot rr\cdot, \cdot\cdot r, \cdot\cdot r$
2	$\cdot r, ll, rr$	$\cdot rr, lll, r\cdot r, \cdot r\cdot$	$\cdot rr\cdot, \cdot\cdot\cdot r, llll, r\cdot r\cdot, \cdot r\cdot r$
3	$\cdot r, ll, ll, r\cdot$	$\cdot rr, lll, lll, rr\cdot$	$\cdot rr\cdot, \cdot\cdot\cdot r, llll, lllll, r\cdot\cdot r, \cdot r\cdot\cdot$
4	$ll, rr, l\cdot$	$\cdot\cdot l, \cdot rr, \cdot rr, ll\cdot, ll\cdot, r\cdot\cdot$	$\cdot\cdot\cdot r, \cdot\cdot ll, \cdot rrr, ll\cdot l, ll\cdot l, rr\cdot\cdot$
5	ll, ll	$\cdot\cdot l, \cdot rr, lll, r\cdot r, l\cdot\cdot$	$\cdot\cdot\cdot r, \cdot\cdot ll, \cdot\cdot ll, \cdot rr\cdot, \cdot rr\cdot, ll\cdot\cdot, \cdot ll\cdot\cdot, r\cdot\cdot\cdot$
6		$ll\cdot, \cdot\cdot l, rrr, l\cdot l$	$\cdot\cdot ll, \cdot rrr, \cdot rrr, lll\cdot, r\cdot r\cdot, l\cdot\cdot\cdot$
7		$ll\cdot, ll\cdot, \cdot\cdot l, \cdot\cdot l$	$\cdot\cdot ll, \cdot rrr, ll\cdot l, r\cdot rr, l\cdot l\cdot$
8			$\cdot\cdot ll, ll\cdot\cdot, rrrr, l\cdot\cdot l, \cdot\cdot l\cdot$
9			$ll\cdot\cdot, ll\cdot\cdot, \cdot\cdot ll, \cdot\cdot ll$

Table 2: The moves for the regular dodecagon.

Sector	Dodecagon
1	$r\cdot\cdot\cdot\cdot, \cdot rr\cdot\cdot, \cdot rr\cdot\cdot, \cdot\cdot\cdot rr, \cdot\cdot\cdot rr$
2	$\cdot rr\cdot\cdot, \cdot\cdot\cdot rr, lllll, r\cdot r\cdot\cdot, \cdot r\cdot\cdot r, \cdot\cdot\cdot r\cdot$
3	$\cdot rr\cdot\cdot, \cdot\cdot\cdot rr, lllll, lllll, r\cdot\cdot\cdot r, \cdot r\cdot r\cdot$
4	$\cdot\cdot\cdot rr, \cdot\cdot lll, \cdot\cdot r\cdot r, ll\cdot ll, ll\cdot ll, r\cdot\cdot r\cdot, \cdot r\cdot\cdot\cdot$
5	$\cdot\cdot\cdot rr, \cdot\cdot lll, \cdot\cdot lll, \cdot rrr\cdot, ll\cdot l\cdot, ll\cdot l\cdot, rr\cdot\cdot\cdot$
6	$\cdot\cdot\cdot\cdot l, \cdot\cdot\cdot rr, \cdot\cdot\cdot rr, \cdot\cdot ll\cdot, \cdot\cdot ll\cdot, \cdot rr\cdot\cdot, \cdot rr\cdot\cdot, ll\cdot\cdot\cdot, ll\cdot\cdot\cdot, r\cdot\cdot\cdot\cdot$
7	$\cdot\cdot\cdot\cdot l, \cdot\cdot\cdot rr, \cdot\cdot lll, \cdot rr\cdot r, \cdot rr\cdot r, lll\cdot\cdot, \cdot r\cdot r\cdot\cdot, l\cdot\cdot\cdot\cdot$
8	$\cdot\cdot\cdot\cdot l, \cdot\cdot ll\cdot, \cdot rrrr, \cdot rrrr, ll\cdot\cdot l, r\cdot r\cdot r, l\cdot l\cdot\cdot$
9	$\cdot\cdot\cdot\cdot l, \cdot\cdot ll\cdot, \cdot rrrr, ll\cdot l\cdot, r\cdot rrr, l\cdot\cdot\cdot l, \cdot\cdot l\cdot\cdot$
10	$\cdot\cdot\cdot\cdot l, \cdot\cdot ll\cdot, ll\cdot\cdot\cdot, rrrrr, l\cdot\cdot l\cdot, \cdot\cdot l\cdot l$
11	$ll\cdot\cdot\cdot, ll\cdot\cdot\cdot, \cdot\cdot ll\cdot, \cdot\cdot ll\cdot, \cdot\cdot\cdot\cdot l, \cdot\cdot\cdot\cdot l$

A. Drawings

In the last few pages of this document we present the drawings that describe the concatenation of diagonal changes moves needed to recover the octagon Farey map.

Let us comment on the pictures that follows. In every picture we represent at the top the quadrangulation Q' together with a line in a generic direction θ inside the appropriate sector. Then we represent the diagonal changes in left to right, top to bottom order. In order to keep the pictures as clear as possible, labels are kept to a minimum and we do not represent the direction θ in the drawings of the staircases moves. Let us remark once again that we will use diagonal changes to approximate the direction θ and *not* the vertical one. With this caveat, the reader can check that all the moves are admisibles,

that is, the staircases are slanted in the appropriate direction. Moreover, in order to save space, we do not represent the final symmetry move in the even numbered sectors.

References

[1] R. Bowen and C. Series, *Markov maps associated with fuchsian groups*, Publ. Math. Inst. Hautes Études Sci. **50** (1979), 153–170.

[2] V. Delecroix and C. Ulcigrai, *Diagonal changes for surfaces in hyperelliptic components: a geometric natural extension of Ferenczi-Zamboni moves*, Geom. Dedicata **176** (2015), 117–174.

[3] G. Forni and C. Matheus, *Introduction to teichmüller theory and its applications to dynamics of interval exchange transformations, flows on surfaces and billiards*, J. Mod. Dyn. **8** (2014), no. 3–4, 271–436.

[4] A. Y. Khinchin, *Continued fractions*, Dover, 1997, Reprint of the 1964 edition by the University of Chicago Press.

[5] M. Kontsevich and A. Zorich, *Connected components of the moduli spaces of abelian differentials with prescribed singularities*, Invent. Math. **153** (2003), no. 3, 631–678.

[6] H. Masur, *Ergodic theory of translation surfaces*, Handbook of dynamical systems. Vol. 1B (Boris Hasselblatt and Anatole Katok, eds.), Elsevier B.V., 2006, pp. 527–547.

[7] C. Series, *The modular surface and continued fractions*, J. Lond. Math. Soc. **31** (1985), 69–80.

[8] C. Series, *Geometrical markov coding of geodesics on surfaces of constant negative curvature*, Ergodic Theory Dynam. Systems **6** (1986), 601–625.

[9] J. Smillie and C. Ulcigrai, *Geodesic flow on the teichmüller disk of the regular octagon, cutting sequences and octagon continued fractions maps*, Dynamical numbers - interplay between dynamical systems and number theory (Martin Möller, Pieter Moree, and Thomas Ward, eds.), Contemp. Math., vol. 532, American Mathematical Society, 2010, pp. 29–65.

[10] J. Smillie and C. Ulcigrai, *Beyond sturmian sequences: coding linear trajectories in the regular octagon*, Proc. Lond. Math. Soc. (3) **102** (2011), no. 2, 291–340.

[11] W. A. Veech, *Teichmüller curves in moduli space, Eisenstein series and an application to triangular billiards*, Invent. Math. **97** (1989), no. 3, 553–583.

[12] J.-C. Yoccoz, *Continued fraction algorithms for interval exchange maps: an introduction*, Frontiers in number theory, physics, and geometry. I (Pierre Cartier, Bernard Julia, Pierre Moussa, and Pierre Vanhove, eds.), Springer, 2006, pp. 401–435.

[13] A. Zorich, *Flat surfaces*, Frontiers in number theory, physics, and geometry. I (Pierre Cartier, Bernard Julia, Pierre Moussa, and Pierre Vanhove, eds.), Springer, 2006, pp. 437–583.
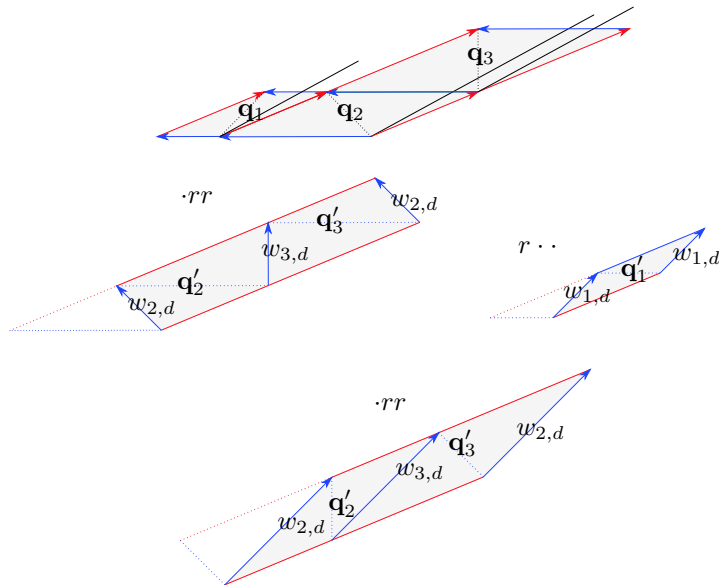
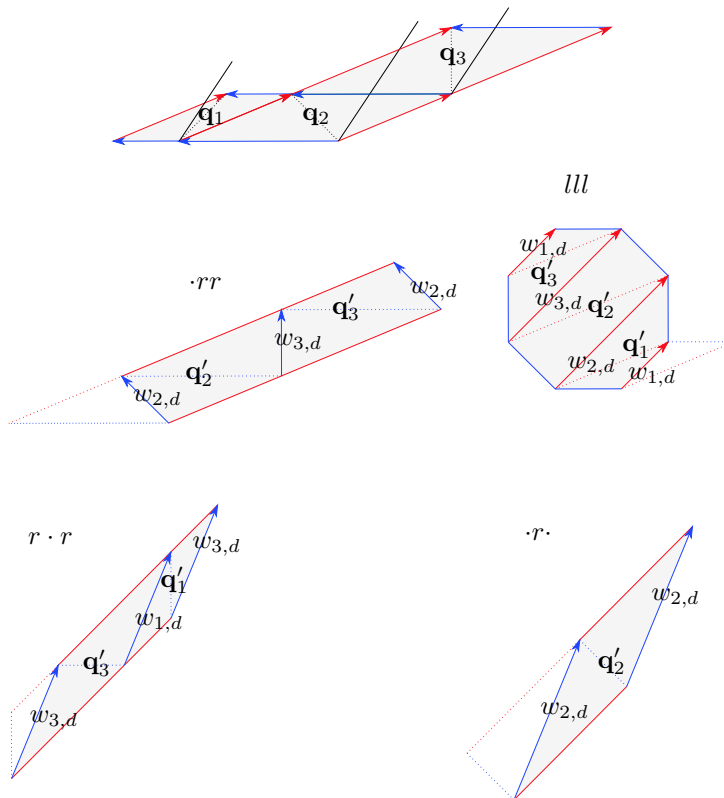Figure 8: The moves of the diagonal changes algorithm for the first sector.

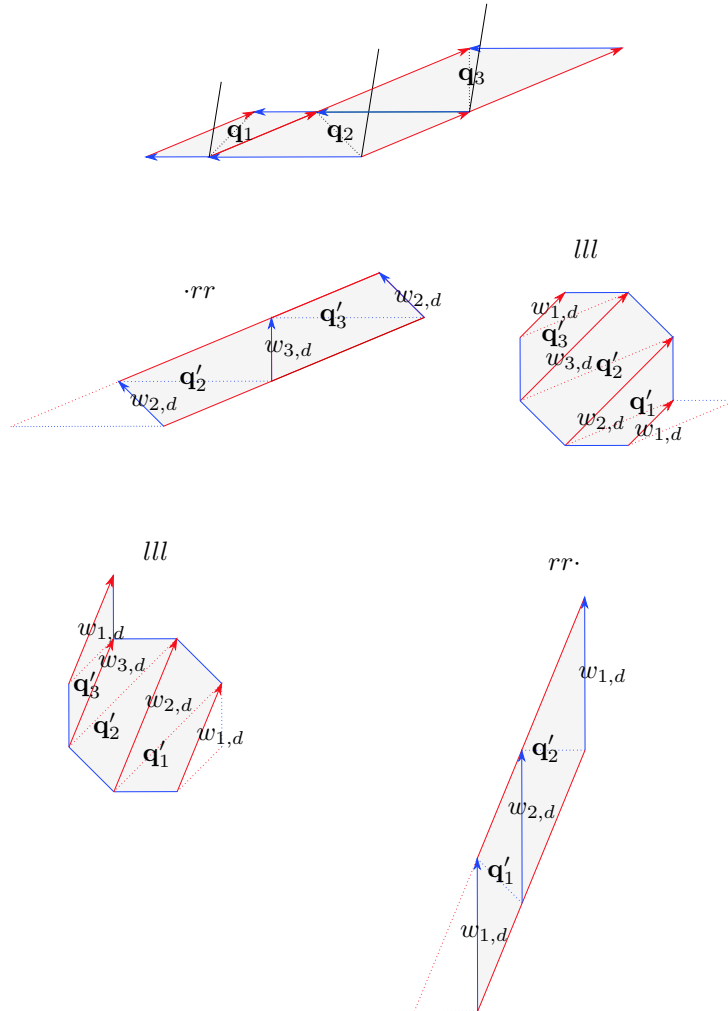Figure 9: The moves of the diagonal changes algorithm for the second sector.

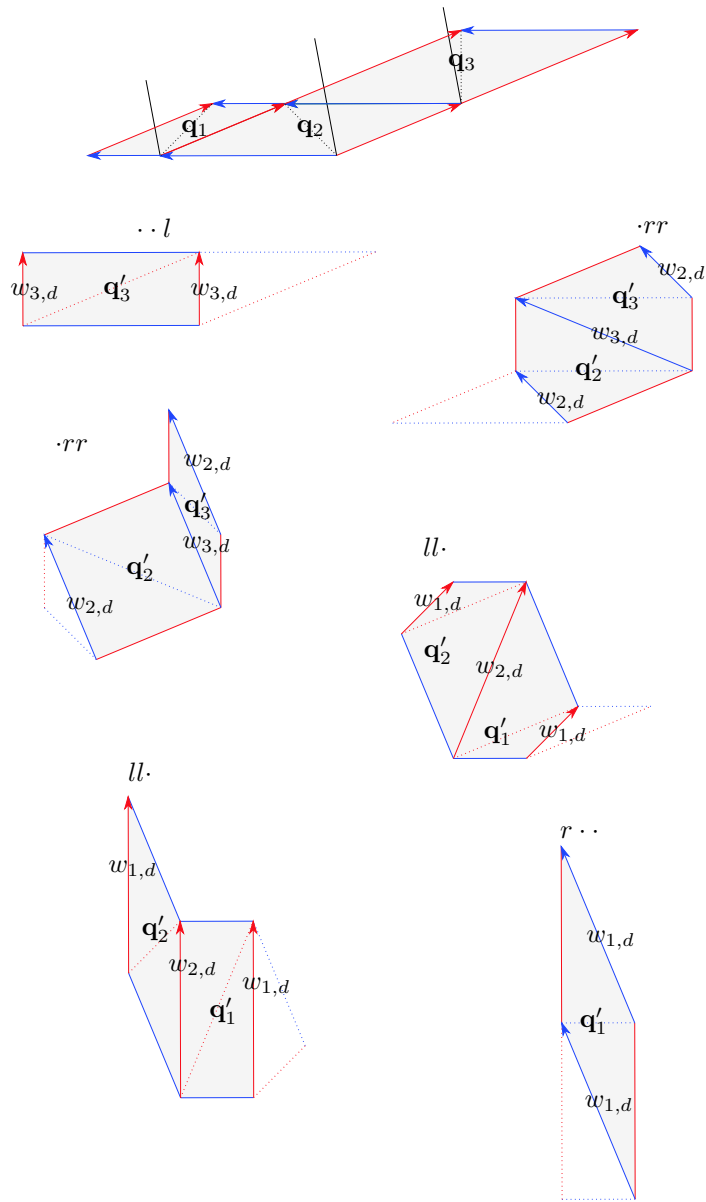Figure 10: The moves of the diagonal changes algorithm for the third sector.

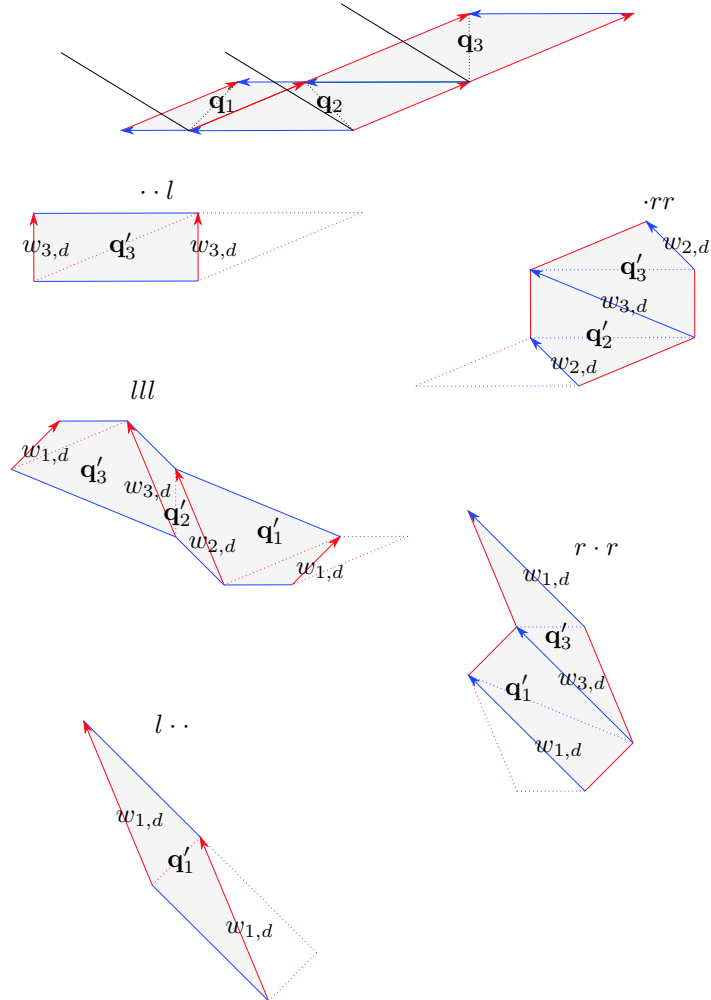Figure 11: The moves of the diagonal changes algorithm for the fourth sector.

Figure 12: The moves of the diagonal changes algorithm for the fifth sector.
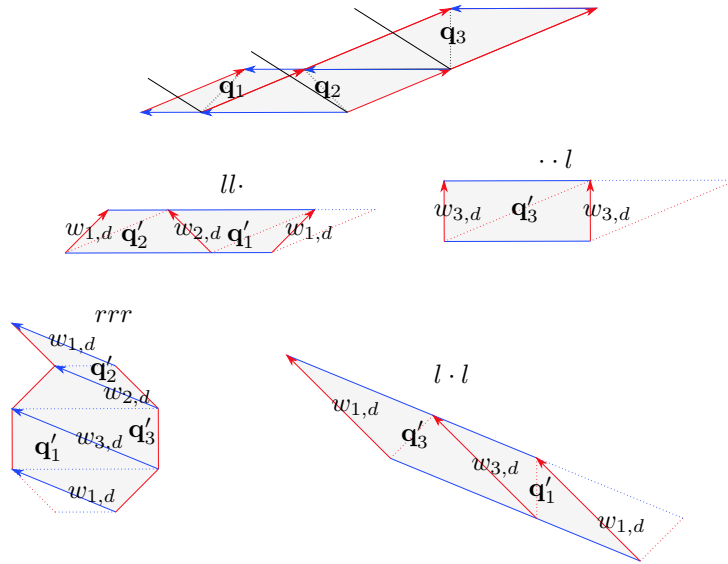
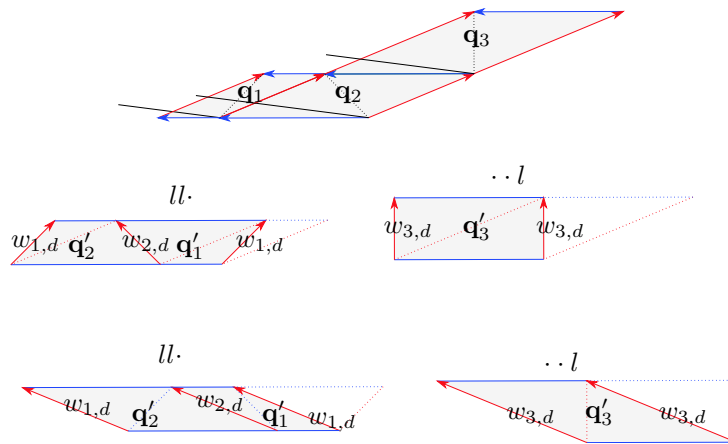Figure 13: The moves of the diagonal changes algorithm for the sixth sector.

Figure 14: The moves of the diagonal changes algorithm for the seventh sector.

Author's address:

Mauro Artigiani
School of Engineering, Science and Technology
Universidad del Rosario
Carrera 6 No. 12 C-16
Bogotá
Colombia
E-mail: `mauro.artigiani@urosario.edu.co`